ELSEVIER

Journal of Alloys and Compounds 425 (2006) 10–13

Journal of ALLOYS AND COMPOUNDS

www.elsevier.com/locate/jallcom

Pressure-induced electrical and magnetic property changes in $CaCuMn_6O_{12}$

W. Zhang, L.D. Yao, L.X. Yang, F.Y. Li, Z.X. Liu, C.Q. Jin, R.C. Yu *

Key Laboratory of Extreme Conditions Physics, Beijing National Laboratory for Condensed Matter Physics, Institute of Physics, Chinese Academy of Sciences, P.O. Box 603, Beijing 100080, PR China

Received 7 December 2005; received in revised form 13 January 2006; accepted 15 January 2006
Available online 21 February 2006

Abstract

$CaCuMn_6O_{12}$ was prepared by using a traditional solid-state reaction method. It is a highly correlated electron system with a small gap appearing at E_F and cluster glass state at low temperature, whereas temperature dependence of resistivity suggests that it is related to thermally activated nearest-neighbor hopping in paramagnetism state in higher temperature range. The resistivity decreases with increasing pressure until 11 kbar, and then increases with further increasing pressure. The blocking temperature T_b goes down under pressure, indicating the suppression of cluster glass state under pressure.

PACS: 75.47.Gk; 91.60.Gf; 75.50.Lk

Keywords: High-pressure; Magnetoresistance; Spin glass

1. Introduction

Recently, a great deal of attention has been attracted to colossal magnetoresistance (CMR) materials not only for their potential application in magnetic sensor, read head and information storage but also for their abundant electronic, magnetic properties and correlation between them. Most of these materials are $Ln_{1-x}A_xMnO_3$ with perovskite structure where Ln is rare earth and A is alkaline earth element. The CMR effect in this kind of material can be explained by double-exchange (DE) mechanism [1], which is that Mn^{3+} and Mn^{4+} ions exchange, e_g electrons via O 2p state. Near T_c local spins are easily aligned by an external field, which enhances electron transfer and results in sharp decrease in resistivity. Their CMR value can be very large, even almost 100%. But these large MR values occur only around the T_C/T_{IM} and at a high magnetic field, which limit their practical application. Room temperature CMR effect was reported for double-perovskite structure Sr_2FeMoO_6 in 1998, which exhibiting intrinsic tunneling-type MR without DE [2]. The CMR effect can't be explained by DE mechanism in another CMR material $Tl_2Mn_2O_7$ either, which has a pyrochlore structure [3]. Recently, the CMR effect was also observed in complex perovskite $CaCu_xMn_{7-x}O_{12}$ compounds [4–6]. The MR effect of $CaCu_xMn_{7-x}O_{12}$ comes from spin polarized inter-grain tunneling, and the MR shows large value at low fields and smoothly increases with decreasing temperature. $CaCu_xMn_{7-x}O_{12}$ represents an $AA'_3B_4O_{12}$ perovskite-like phase with cell parameters of twice of an ideal perovskite. A is generally a large monovalent, divalent or rare earth cation, A′ is Cu^{2+} or Mn^{3+}, and B can be $Mn^{4+/3+}$. The $CaCu_xMn_{7-x}O_{12}$ shows ferromagnetic state below 355 K when $x=3$ and the ferromagnetic interaction in $CaCu_xMn_{7-x}O_{12}$ weakens with increasing x. It should be noted that Jahn-Teller ions can occupy both A′ and B sites while non-Jahn-Teller ions Mn^{4+} only occupy at B site. In this paper we show some physical properties of well-crystallized $CaCuMn_6O_{12}$ without any impurity.

2. Experimental

The polycrystalline $CaCuMn_6O_{12}$ was prepared by using a traditional solid-state reaction method. CaO, CuO, MnO_2, and $KClO_4$ (30% in weight added as mineralizer) were mixed thoroughly in stoichiometric ratios in an agate mortar and pressed into pellets [7,8]. The pellets were sintered at 850 °C for 10 h

* Corresponding author. Tel.: +86 10 82649159; fax: +86 10 82649531.
E-mail address: rcyu@aphy.iphy.ac.cn (R.C. Yu).

0925-8388/$ – see front matter © 2006 Elsevier B.V. All rights reserved.
doi:10.1016/j.jallcom.2006.01.040

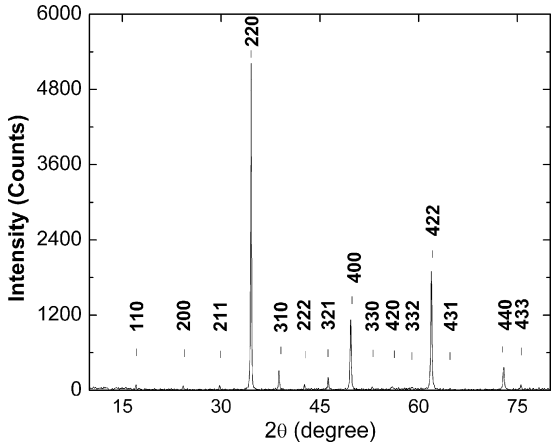

Fig. 1. XRD of $CaCuMn_6O_{12}$. All peaks can be indexed with Im-3, even very little one.

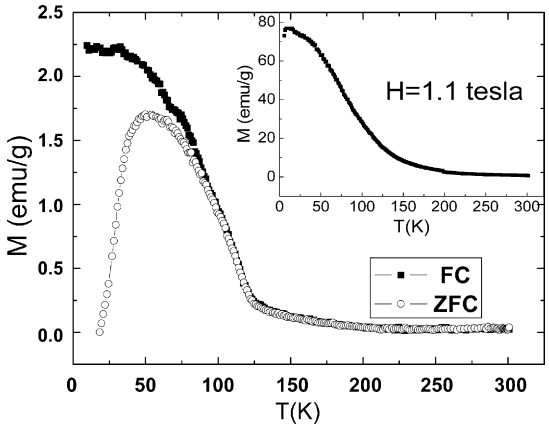

Fig. 2. Magnetization vs. temperature for $CaCuMn_6O_{12}$ sample. Both zero-field-cooled (ZFC) and field-cooled (FC) measure were under the magnetic fields $H = 0.01$ T. The inset shows magnetization vs. temperature under 1.1 T field.

in an oxygen flow. The room temperature X-ray diffraction (XRD) measurements were performed using a M18AHF diffractometer with Cu Kα. Clamp-type piston cylinder cell is used to measure temperature dependence of resistivity at different hydrostatic pressures. Resistivity was measured with the standard four-probe technique. Electrical contacts were established using silver paint on a bar-shaped sample (∼1.25 mm × 1.4 mm × 3.9 mm). The sample temperature was monitored with aluminonickel and chromel thermocouple placed near the sample and a mixture of silicone oil and kerosene (1:1) as a pressure-transmittting medium. In our experiments, the sample was separated from the pressure transmitting medium by an insulator layer painted on the sample. All the pressure values quoted in this paper were measured at room temperature. Magnetic moment versus temperature was measured using a Mag Lab System (2000 Oxford UK).

3. Results and discussion

3.1. Structure

Fig. 1 shows the X-ray diffraction pattern of $CaCuMn_6O_{12}$ and no impurity was detected. $KClO_4$ was decompounded to KCl and O_2 at 600 °C, and all the KCl was vaporized away during sintering at 850 °C for 10 h in oxygen flow. All the peaks in the XRD can be indexed by a cubic structure with a space group Im-3. It should be noted that in this structure the bond angle of Mn–O–Mn at B site is 141.18° instead of 180°, as in the ideal perovskite structure. Electron microscopy studies were also carried out on this sample and the results are consistent with the XRD data.

3.2. Magnetic properties and electrical properties

3.2.1. Magnetic properties

$CaCu_3Mn_4O_{12}$ shows ferromagnetic below 355 °C and the magnetic moments of Mn ions at B site are ferromagnetically arranged while Cu^{2+} ions at A site are antiferromagnetically arranged with the Mn ions [6,9]. So the more Mn^{3+} ions substitute for Cu^{2+}, the more antiferromagnetic coupling competes with the ferromagnetic. Fig. 2 shows the temperature dependence of DC magnetization of $CaCuMn_6O_{12}$ measured at a field of 0.01 T during warming process, after being zero field cooled (ZFC) and field cooled (FC 0.01 T) from room temperature to 5 K. The inset is the temperature dependence of DC magnetization at 1.1 T in order to compare with other reported results. It should be noted that at a higher field of 1.1 T, we also got the same curve as reported in Ref [5]. The magnetization behavior at low field is different from that at 1.1 T as shown in Fig. 2. At higher temperature range, the FC and ZFC curves are superposed and show no difference between them. The magnetizations are very small and decrease smoothly with increasing temperature, indicating a paramagnetic state. With descending temperature, there is a deviation between them. At low temperature, the ZFC curve has a cusp whereas the magnetization keeps increasing with decreasing temperature for FC curve. Fig. 3 shows the M–H curves at 5 and 260 K, respectively. At 260 K, the magnetization is very small, consisting with the paramagnetic state behavior. At 5 K, the magnetization increases sharply at low field and tends to saturation. With further increasing magnetic field, the magnetization increases a little, indicating the saturation is still not reached. From the above results, it is suggested that at low temperature $CaCuMn_6O_{12}$ is a cluster glass state without long range ferromagnetic order. T_b represents the temperature that spins freeze at random directions, which is obtained from the dM/dT

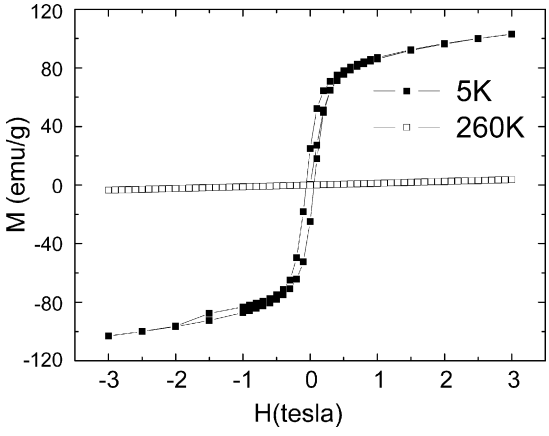

Fig. 3. Magnetization vs. field for $CaCuMn_6O_{12}$ sample at 5 and 260 K.

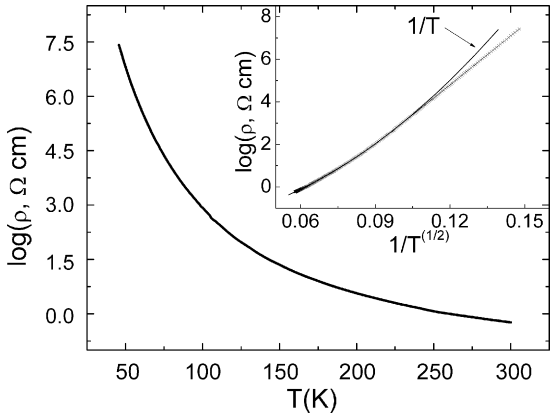

Fig. 4. Resistivity vs. temperature behavior for $CaCuMn_6O_{12}$ sample. The inset shows $\log(\rho) \propto (1/T)^{1/2}$ at low temperature, and $\log(\rho) \propto (1/T)$ at high temperature.

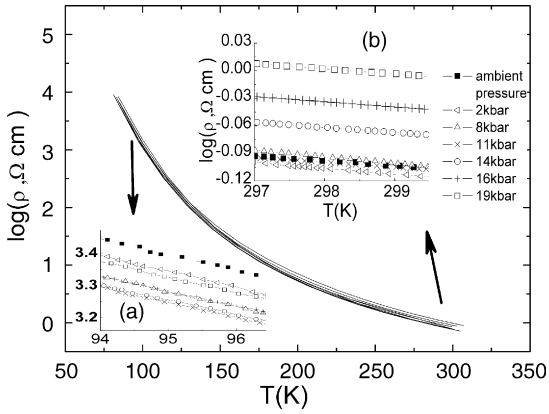

Fig. 5. Resistivity vs. temperature at different pressures (0, 8, 11, 14, 16, 19 kbar). The inset *a* is detail of curves at low temperature. The inset *b* is detail of curves at high temperature.

(ZFC) curve, and is determined as 114 K. In the $CaCuMn_6O_{12}$ all the Mn ions at A′ site are Mn^{3+}, while Mn^{3+} and Mn^{4+} are arranged with equal amount at B site, but distribute irregularly. Comparing with Mn–O–Mn angle-180° in an ideal perovskite, the Mn–O–Mn in $CaCuMn_6O_{12}$ is 141.18°. The bending of Mn–O–Mn bond weakens DE interaction between Mn^{3+} and Mn^{4+} at B sites and is unfavorable for ferromagnetic state. In the super-exchange interaction between the same valence Mn ions, the angle 180° of Mn–O–Mn favors antiferromagnetism and the angle 90° of Mn–O–Mn favors ferromagnetism when the Mn ions have same orbital directions. If the Mn ions have perpendicular orbital directions, the bond angle 180° favors ferromagnetism [10]. In a word, there may be ferromagnetic or antiferromagnetic configurations at different complex conditions, but the bond angle 141.18° is favor neither ferromagnetic nor antiferromagnetic couplings. This results in weak coupling among the cluster spin states. So it is reasonable to increase magnetic frustration and cluster glass state and increase residual resistivity [11].

3.2.2. Electrical properties

Most of CMR materials $Ln_{1-x}A_xMnO_3$ show metal behavior below their T_C around $x = 0.3$ (Mn^{4+}:$Mn^{3+} \sim 3{:}7$) and semiconductor behavior around $x = 0.5$ (Mn^{4+}:$Mn^{3+} \sim 1{:}1$) due to charge ordering and weak DE interaction. The resistivity measurements of $CaCuMn_6O_{12}$ (shown in Fig. 4) indicate that $CaCuMn_6O_{12}$ is a semiconductor. As a highly correlated electron system, at low temperature (45 K < T < 100 K), $CaCuMn_6O_{12}$ has a small gap appearing at E_F because the resistivity is in accordance with Mott's law for variable range hopping and the hopping law is $\log(\rho) \propto (1/T)^{1/2}$ [12]. At high temperature ($T > 100$ K), the carriers form small dielectric polarons and the temperature dependence of resistivity follows thermally activated nearest-neighbor hopping, i.e., $\log(\rho) \propto (1/T)$ [13]. The exact turning point of two parts was determined as 113.3 K through anatomizing the inset of Fig. 4, which accords with the blocking temperature T_b. It suggests that the resistivity of $CaCuMn_6O_{12}$ versus temperature is $\log(\rho) \propto (1/T)^{1/2}$ for cluster glass state while $\log(\rho) \propto (1/T)$ for paramagnetic state.

3.3. Pressure effects on electrical properties and blocking temperature

3.3.1. Resistivity change with pressure

Fig. 5 shows temperature dependence of resistivity curves at different pressures. The enlarged details at low temperature and room temperature are shown in the inset (a) and (b), respectively. *PR* is defined as $PR = [\rho(P) - \rho(0)]/\rho(0)$, where $\rho(P)$ and $\rho(0)$ denotes resistivities at pressure P and ambient pressure, respectively. Fig. 6 represents *PR* versus pressure at different temperatures. The resistivity keeps nearly the same until 11 kbar at 300 k, but it increases linearly above 11 kbar. The maximum *PR* value is 25.85% at 19 kbar. At 95 K, the resistivity decreases with pressure below 11 kbar, while increases with pressure above 11 kbar as the same trend at 300 K. The minimum *PR* value is −29.1%. At moderate temperatures 200 and 150 K, the *PR* behaviors are between the behaviors at 95 and 300 K. In a word, the resistivity decreases from ambient pressure to 11 kbar more or less and increases from 11 to 19 kbar. We studied the crystal structure stability of $CaCuMn_6O_{12}$ under pressure using X-ray diffraction with synchrotron radiation and observed no crystal structural change around 11 kbar [14]. These phenomena indicate that there might be two different electronic structures below and above 11 kbar, which results in a concave in the *PR* versus pressure curves (Fig. 6).

3.3.2. Blocking temperature change with pressure

The blocking temperatures T_b at different pressures were picked up from Fig. 5, and are shown in Fig. 7. Below 11 kbar, the T_b decreases a little with increasing pressure except the first point. We think this deviation from the decreasing trend is caused by the effect of loading pressure from the ambient. With increasing pressure form 11–14 kbar, the T_b decreased from 113.5 to 102.8 K and then decreases smoothly with further increasing pressure up to 19 kbar. These indicate that the pressure suppresses cluster glass state from paramagnetic state. It should be pointed out that we also repeated the measurements of temperature dependence of resistivity under high pressure using another pressure transmitting medium and obtained the same results,

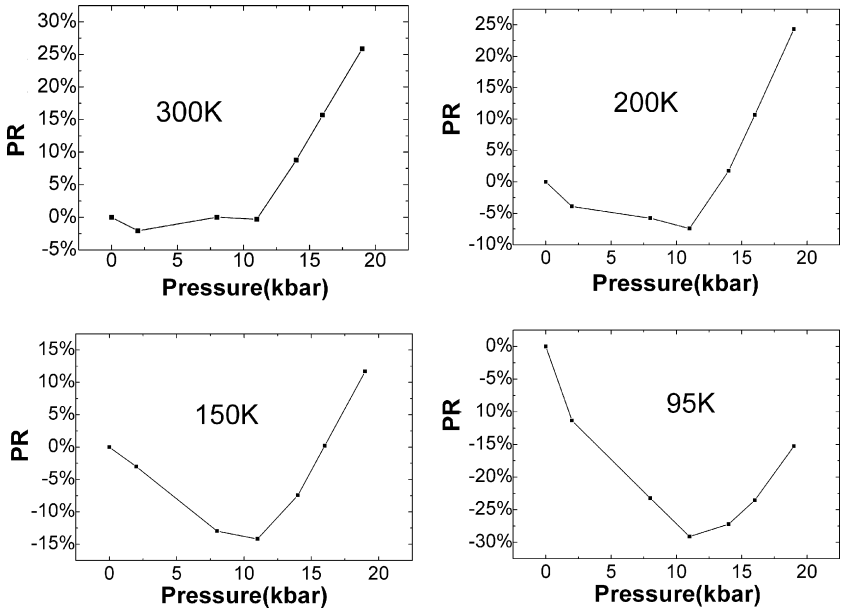

Fig. 6. *PR* vs. pressure at different temperatures (300, 200, 100, 95 K).

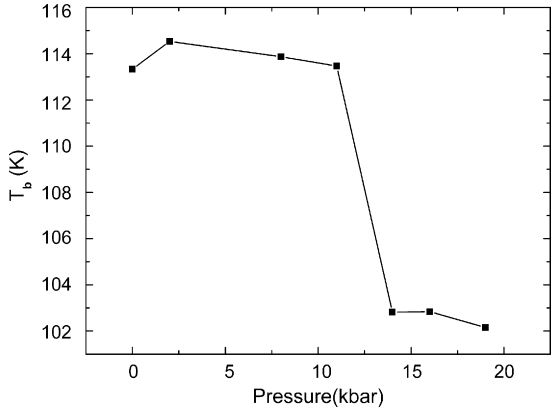

Fig. 7. The pressure dependence of the T_b.

which indicate that the phenomena we obtained under pressures are from materials we studied, not from the pressure transmitting medium.

4. Conclusions

$CaCuMn_6O_{12}$ polycrystalline sample was synthesized by a traditional solid-state reaction method. The temperature dependence of resistivity and temperature dependence of magnetization show that $\log(\rho) \propto (1/T)^{1/2}$ corresponds to cluster glass state at low temperature while $\log(\rho) \propto (1/T)$ corresponds to paramagnetic state. The blocking temperature T_b decreases with increasing pressure and descends 10 K from 11 to 14 kbar, which means that the pressure suppresses cluster glass state. The resistivity of $CaCuMn_6O_{12}$ decreases more or less below 11 kbar, whereas increases above 11 kbar up to 19 kbar, which means there might be an electronic structural change around this pressure point.

Acknowledgements

This work was supported by the National Natural Science Foundation of China (Grant Nos. 50471053, 10274099, 50321101 and 50332020) and the State Key Development Program for Basic Research of China (Grant No. 2005CB623602 and 2005CB724402).

References

[1] C. Zener, Phys. Rev. 82 (1951) 403.
[2] K.L. Kobayashi, T. Kimura, H. Sawada, K. Terakura, Y. Tokure, Nature (London) 395 (1998) 677.
[3] Y. Shimakawa, Y. Kubo, T. Manako, Nature (London) 379 (1996) 53.
[4] Z. Zeng, M. Greenblatt, M.A. Subramanian, M. Croft, Phys. Rev. Lett. 82 (1999) 3164.
[5] I.O. Troyanchuk, L.S. Lobanovsky, N.V. Kasper, M. Hervieu, A. Maignan, C. Michel, H. Szymczak, A. Szewczyk, Phys. Rev. B. 58 (1998) 14903.
[6] Z. Zeng, M. Greenblatt, J.E. Sunstrom, M. Croft IV, S. Khalid, J. Solid State Chem. 147 (1999) 185–198.
[7] E.A. Pomerantseva, D.M. Itkis, E.A. Goodilin, J.G. Noudem, M.V. Lobanov, M. Greenblatt, Yu.K. Tretyakov, J. Mater. Chem. 14 (2004) 1150.
[8] J.A. Alonso, J. Sanchez-Benitez, A. De Andres, M.J. Martinez-Lope, M.T. Casais, J.L. Martinez, Appl. Phys. Lett. 83 (2003) 2623.
[9] B. Bochu, J.C. Joubert, A. Collomb, B. Ferrand, D. Samaras, J. Magn. Magn. Mater. 15 (1980) 1319.
[10] E. Dagotto, T. Hotta, A. Moreo, Phys. Rep. 334 (2001) 1.
[11] J.L. Garcia-Munoz, J. Fontcuberta, B. Martinez, A. Seffar, S. Pinol, X. Obradors, Phys. Rev. B. 55 (1997) R668.
[12] J.M.D. Coey, M. Viret, S. von Molnar, Adv. Phys. 48 (1999) 167.
[13] P.H. Wagner, V. Metlushko, L. Trappeniers, A. Vantomme, J. Vanacken, G. Kido, V.V. Moshchalkov, Y. Bruynseraede, Phys. Rev. B. 55 (1997) 3699.
[14] W. Zhang, et al., to be submitted.